Collective Effects in Linear Spectroscopy of Molecular Aggregates

A. A. Kocherzhenko[1], J. Dawlaty[2], B. P. Abolins[1], F. Herrera[3,4], D. B. Abraham[5], K. B. Whaley[1]
[1] *Department of Chemistry, University of California, Berkeley, CA 94720*
[2] *Department of Chemistry, University of Southern California, Los Angeles, CA 90089*
[3] *Department of Chemistry and Chemical Biology, Harvard University, Cambridge, MA 02138*
[4] *Department of Chemistry, Purdue University, West Lafayette, IN 47907*
[5] *Department of Theoretical Physics, University of Oxford, UK*
(Dated: July 9, 2013)

A consistent analysis of linear spectroscopy for arrays of dipole-coupled two-level molecules reveals distinct signatures of weak and strong coupling regimes separated by a critical point. Multiple molecular excitations (odd(even) in weak(strong) coupling) are accessed from the ground state. As the coupling increases, the single excitation oscillator strength rapidly exceeds the Heitler-London value and diverges at the critical point, returning to a quadratic size scaling in strong coupling, where also the photon frequency decreases with size. The lowest accessible excitation is found to show a one-photon hyperradiance.

PACS numbers: 64.70.Tg, 71.35.Cc

Quantum correlations between light-absorbing pigments can enhance light-matter interaction, resulting in superradiance, i.e., in anomalously fast spontaneous emission [1, 2]. In most materials where superradiance is observed, the interaction energy between chromophores is smaller than the single-chromophore excitation energy. We show that systems with stronger interactions between chromophores can form a correlated quantum phase, separated from the weak interaction regime by a quantum critical point. This correlated phase exhibits qualitatively new spectroscopic properties, including one-photon hyperradiance for the lowest excited state. Development of materials that possess such properties opens new prospects for the efficient capture and sensing of light.

Consider a one-dimensional ($d = 1$) array of M 2-level chromophores with excitation energy ε that are coupled by dipole-dipole interactions b between nearest neighbors. This system is described by the Hamiltonian of Krugler, Montgomery and McConnell (KMM) [3]:

$$H = \sum_{m=1}^{M} \left[\varepsilon P_m^\dagger P_m + b \left(P_m^\dagger + P_m \right) \left(P_{m+1}^\dagger + P_{m+1} \right) \right]. \tag{1}$$

Here $P_m^\dagger$ creates and P_m annihilates an excitation at site m (we work with unit lattice spacing). These operators are a product of a pair of electron creation and annihilation operators in the molecular basis. Since charge transfer is not allowed, pairs of the operators $P_m^\dagger$, P_m commute off site; on site we have $P_m^\dagger P_m + P_m P_m^\dagger = 1$. Regarding P_m as a spin lowering operator for a chain of spin-1/2 entities, i.e., $P_m^\dagger + P_m = \sigma_m^x$, leads, in the usual Pauli notation, to the equivalent quantum Ising Hamiltonian $H_{\text{spin}} = \varepsilon \sum_{m=1}^{M} (1 + \sigma_m^z)/2 + b \sum_{m=1}^{M} \sigma_m^x \sigma_{m+1}^x$.

With a few exceptions limited to relatively weak coupling [4–6], studies of excitonic energy transfer and spectroscopy of dipolar molecular aggregates tend to omit the double excitation and deexcitation terms, $P_m^\dagger P_{m+1}^\dagger$ and $P_m P_{m+1}$, in Eq. (1). This "Heitler-London" (HL) approximation reproduces experimental absorption spectra reasonably well for $|b| \ll \varepsilon$. However, KMM [3] showed that it is inconsistent to neglect these terms and that they result in collective effects that lead to changes in the structure of the ground and excited eigenstates of Eq. (1). This motivates us to revisit Eq. (1) with new emphasis on its spectroscopic implications and with particular focus on the hitherto unexplored consequences of the many-body nature of the Hamiltonian eigenstates for spectroscopy in the regime of strong coupling, $B = 2|b|/\varepsilon > 1$, where B is the scaled coupling. We show that a consistent analysis gives rise to unique spectroscopic signatures that are forbidden in the HL approximation and that become dominant as B increases.

Since the eigenstates of Eq. (1) are critical for our spectroscopic analysis, we first summarize the key features of the analytic diagonalization by KMM [3]. The first step is a Jordan-Wigner transformation of $\{P_m\}$: $f_1 = P_1$, $f_m = Q_{m-1} P_m$, $Q_m = \prod_{j=1}^{m} \left(1 - 2P_j^\dagger P_j\right)$, for $2 \le m \le M$. The operators $\left\{f_m, f_m^\dagger\right\}$ have lattice-fermionic anti-commutation relations, so Eq. (1) becomes a quadratic form in fermions, except for the boundary term, which gives the expected form in fermions, but multiplied by $-Q_M$. Since $[H, Q_M] = 0$, the Hamiltonian can be decomposed into two quadratic forms, H_+ and H_-, by projection onto orthogonal subspaces: $H = Q_+ H_+ + Q_- H_-$, where $Q_\pm = (1 \pm Q_M)/2$. H_+ and H_- are then diagonalized separately, after applying a discrete Fourier transformation: $F^\dagger(k) = M^{-1/2} \sum_{m=1}^{M} e^{ikm} f_m^\dagger$, where for $H_\pm$: $e^{ikM} = \mp 1$, $0 \le k < 2\pi$. The allowed values of the wavenumber k are denoted $\alpha = 2\pi(m-1)/M$ for H_- and $\beta = \pi(2m-1)$ for H_+. The Bogoliubov-Valatin transformation $G^\dagger(k) = \cos\theta(k) F^\dagger(k) - i \sin\theta(k) F(-k)$ diagonalizes $H_+(H_-)$ for $k = \beta(\alpha)$, yielding

$$H_\pm = E_\pm + \sum_{k:\ \exp(ikM) = \mp 1} E(k)\, G^\dagger(k)\, G(k), \tag{2}$$

where $\tan\theta(k) = (2b\sin k)^{-1}[E(k) - E_0(k)]$, $E(k) = \left[E_0(k)^2 + 4b^2\sin^2 k\right]^{1/2}$ and $E_0(k) = \varepsilon + 2b\cos k$ is the HL dispersion relation. The ground states $|\Phi_\pm\rangle$ of $H_\pm$ resemble the Bardeen-Cooper-Schrieffer (BCS) ground state and have energies $E_\pm = -\sum[E(k) - E_0(k)]/2$, where the summation is over all allowed k values [3]. All eigenstates of Eq. (1) are then given by the eigenstates of H_+ produced by applying an even number of $G^\dagger(\beta)$ operators to $|\Phi_+\rangle$, together with the eigenstates of H_- produced by applying an odd ($B < 1$) or even ($B > 1$) number of $G^\dagger(\alpha)$ operators to $|\Phi_-\rangle$ [7]. The ground state of H is always $|\Phi_+\rangle$.

A key insight of KMM was to suggest that for $B > 1$ the ground state of the Hamiltonian, Eq. (1), exhibits either ferroelectric or anti-ferroelectric polarization. Given the mapping to $H_{\rm spin}$ [8], we expect that this ordered state is stable against quantum fluctuations and that this regime is separated by a quantum critical point at $B = 1$ from a disordered regime with no intrinsic polarization at weak couplings. From now on we will restrict our attention to the case $b < 0$ [9].

Consider the interaction of such an array with light, in the electric dipole approximation. Since the dipole excitation operator $\sigma_m^x = P_m^\dagger + P_m$ anti-commutes with parity, some immediate predictions about the linear spectra of the chromophore assemblies studied can be made. First, the ground state is coupled to *all* states of opposite parity, while in the HL approximation the only allowed transitions are to single-excitation states [4, 5]. Second, for $B > 1$ it can be seen by the residue theorem that the lowest energy excitation is $E_- - E_+ \propto M^{1/2}\exp(-M\kappa)$, $\cosh\kappa = (1+B^2)/2B$, which goes to zero for all B values as $M \to \infty$. Provided the matrix element for this transition is non-zero, photon absorption at arbitrarily low frequencies is expected for an array of strongly coupled chromophores. This is in stark contrast to the HL description that predicts an incorrect energy spectrum and no allowed low-energy transition for $B > 1$.

We now describe the calculation of transition matrix elements in this strong coupling regime. Without loss of generality, we restrict our attention to $\langle\Phi_-|\,G(\alpha_{2n})\ldots G(\alpha_1)\,\sigma_1^x\,|\Phi_+\rangle$, since all allowed excitations may be generated from σ_1^x by making use of the translational symmetry of Eq. (1): $TP_mT^\dagger = P_{m-1}, 2 \le m \le M$ with $TP_1T^\dagger = P_M$. In the strong coupling regime, the Hamiltonian ground state, $|\Phi_+\rangle$, has even parity and the ground state of H_-, $|\Phi_-\rangle$, has odd parity. Consequently, the allowed optical transitions from $|\Phi_+\rangle$ are to $|\Phi_-\rangle$ and to states with an even number of excitations generated from the latter state, with corresponding transition dipole moments $\langle\Phi_-|\,G(\alpha_{2n})\ldots G(\alpha_1)\,\sigma_1^x\,|\Phi_+\rangle$. Using an extension of Wick's theorem [10], these matrix elements can be shown to satisfy

$$\sum_{\alpha_1}(\alpha_1,\beta)_1\,\langle\Phi_-|\,G(\alpha_{2n})\ldots G(\alpha_1)\,\sigma_1^x\,|\Phi_+\rangle = \sum_{j=2}^{2n}(-1)^{j-1}(-\alpha_j,\beta)_2\Delta_{1j}\,\langle\Phi_-|\,G(\alpha_{2n})\ldots G(\alpha_1)\,\sigma_1^x\,|\Phi_+\rangle\,, \qquad (3)$$

$(\alpha,\beta)_l = \left[e^{i\theta_{\beta,\alpha}}e^{i(\alpha-\beta)} - (-1)^l e^{-i\theta_{\beta,\alpha}}\right]/M\left[e^{i(\beta-\alpha)} - 1\right]$, $l = 1, 2$, where $\theta_{\beta,\alpha} = \theta(\beta) - \theta(\alpha)$, $\theta(k)$ is defined above and Δ_{1j} denotes removing the operators $G(\alpha_1)$ and $G(\alpha_j)$ from the matrix element that follows it. Eq. (3) can be solved analytically for $M \to \infty$ using the methods of [11] and numerically for finite systems as follows. Setting $n = 1$ in Eq. (3) and dividing both sides by $\langle\Phi_-|\,\sigma_1^x\,|\Phi_+\rangle$ results in a set of M^2 linear equations with complex coefficients

$$\sum_{\alpha_1}(\alpha_1,\beta)_1 K(\alpha_1,\alpha_2) = (-\alpha_2,\beta)_2, \qquad (4)$$

which can be grouped into M sets (indexed by α_2) with M linear equations (indexed by β) in each set. Each set is equivalent to a matrix equation for a column of the matrix $K(\alpha_1,\alpha_2) = \langle\Phi_-|\,G(\alpha_2)\,G(\alpha_1)\,\sigma_1^x\,|\Phi_+\rangle\,/\,\langle\Phi_-|\,\sigma_1^x\,|\Phi_+\rangle$ with fixed index α_2, that can be solved by gaussian elimination using an LU factorization [12]. The denominator $\langle\Phi_-|\,\sigma_1^x\,|\Phi_+\rangle$ is determined by a completeness argument

$$1 = |\langle\Phi_-\,|\sigma_1^x|\,\Phi_+\rangle|^2\det(I + X)\,, \qquad (5)$$

where I is the identity and X is an $M \times M$ real matrix linearly related to K [7]. Solution of Eqs. (4) and (5) completely defines the matrix element $\langle\Phi_-|\,G(\alpha_2)\,G(\alpha_1)\,\sigma_1^x\,|\Phi_+\rangle$. Higher-order matrix elements can then be calculated recursively, using the Pfaffian type solution [11] generated by Eq. (3). The solution is thus an algorithm that relates $2n$-particle matrix elements to ones with $2n-2$ particles. Iterating n times yields a sum of products of n contraction functions, resulting in a generalized form of Wick's theorem in which the in and out states are expressed naturally in terms of two different representations of the underlying Hilbert space. The algorithm is polynomial in the system size M, which significantly improves over the exponential scaling of directly diagonalizing Eq. (1) [13]. To our knowledge this is the first use of such a technique for obtaining exact solutions for finite sizes.

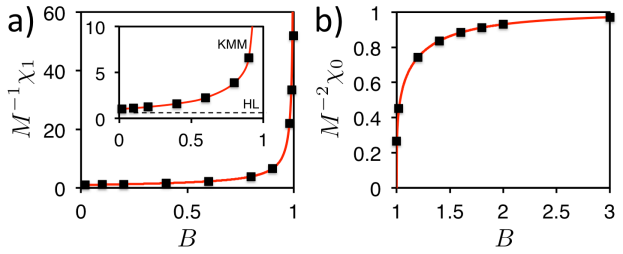

FIG. 1: Total oscillator strength a) χ_1 vs B for excitation to the one-excitation manifold in weak coupling ($B < 1$), and b) χ_0 vs B for excitation to the lowest excited state in strong coupling ($B > 1$), for a system of size $M = 200$ (black squares) and $M \to \infty$ (red lines). Inset: comparison of χ_1 from KMM with values from HL.

The matrix elements $\langle\Phi_-|G(\alpha_{2n+1})\ldots G(\alpha_1)\,\sigma_1^x|\,\Phi_+\rangle$ in the weak coupling regime, $B < 1$, can be calculated using a similar procedure or, alternatively, obtained directly from the matrix elements in the strong coupling regime using a duality transformation [7].

This approach now allows a consistent calculation of the linear spectra of dipole-coupled molecular arrays for any coupling strength B. We first consider the total oscillator strength χ_i for transitions from the ground state to the lowest set of excitations i. In the weak coupling regime, the lowest energy dipole-allowed transitions are from $|\Phi_+\rangle$ to one-excitation states and we have $\chi_1 = \sum_\alpha \left|\langle\Phi_-|\,G(\alpha)\sum_{m=1}^M \sigma_m^x\,|\Phi_+\rangle\right|^2$. In the strong coupling regime, the lowest energy transition is from $|\Phi_+\rangle$ to $|\Phi_-\rangle$ and we have $\chi_0 = \left|\langle\Phi_-|\sum_{m=1}^M \sigma_m^x\,|\Phi_+\rangle\right|^2$. These expressions can be simplified using the translational symmetry of Eq. (1) and explicitly evaluated using the matrix elements for finite M derived above. The results are shown by black squares in Figure 1. Solutions for $M \longrightarrow \infty$ may be obtained using the analytic methods of Ref. [10], yielding $\lim_{M\to\infty} M^{-1}\chi_1 = (1-B)^{-\frac{3}{4}}(1+B)^{\frac{1}{4}}$ and $\lim_{M\to\infty} M^{-2}\chi_0 \to \left(1-1/B^2\right)^{\frac{1}{4}}$. These solutions reveal the size scalings $\chi_1 \propto M$, $\chi_0 \propto M^2$ and are plotted as red lines in Figure 1. We find excellent agreement with the finite-size values for $M = 200$ everywhere except very close to the critical point $B = 1$ [7], where in the infinite size limit χ_1 diverges and χ_0 goes to 0.

Our analysis shows that only the lowest excited state, $\alpha = 0$, contributes to the oscillator strength χ_1, while χ_0 is determined by the single transition from $|\Phi_+\rangle$ to $|\Phi_-\rangle$. The lowest excited state possesses a one-photon superradiance [14] scaling as M for $B < 1$ (including the HL limit [15]) and as M^2 for $B > 1$. Furthermore, the superradiance of this state is also strongly dependent on B, rapidly increasing above the HL value as B increases and diverging as the critical point is approached from below. In the strong coupling regime $M^{-2}\chi_0$ is asymptotic to 1 as $B \to \infty$, implying that here the excited state $|\Phi_-\rangle$ is superradiant with a rate $\propto M^2$ equal to the maximum possible for non-interacting systems [16] and hence it constitutes a one-photon hyperradiant state [17]. We note that this superradiance derives from the dipolar interactions within the array rather than from interaction with the radiation field. The manifestation of superradiance that is M^2-dependent in the strong coupling regime and divergent at the critical point is quite remarkable, given that in both situations it is associated with a single excitation. Both critically and strongly coupled arrays would therefore display extremely fast and high intensity photon emission.

We already specified that in the limit $M \to \infty$, $M^{-1}\chi_1$ diverges as $B \to 1-$. It is informative to analyze this quantity as a fluctuation sum of pair correlations of transition dipole moments, $C(m-n) = \sum_\alpha \langle\Phi_+|\,\sigma_m^x G^\dagger(\alpha)\,|\Phi_-\rangle\,\langle\Phi_-|\,G(\alpha)\sigma_n^x\,|\Phi_+\rangle$ ($B < 1$), for which the correlation propagates solely through single excitations. Carrying out the sum over α and then using translational symmetry, we find $\lim_{M\to\infty} M^{-1}\chi_1 = C(0) + 2\sum_{m=1}^\infty C(m)$, with

$$C(m) = \frac{(1-B^2)^{1/4}}{2\pi}\int_0^{2\pi} dk \frac{e^{imk}}{(1+B^2-2B\cos k)^{1/2}}.$$

Asymptotically for large M, we see that there is a length scale $(1-B)^{-1}$, which diverges at the quantum critical point. In contrast, for the HL model, we have $C(m) = \delta_{mn}$. Thus not only does HL underestimate the oscillator strength and hence superradiance for $B < 1$, it also shows no divergence at the critical point (see inset in Figure 1a). HL is furthermore inapplicable in the strong coupling regime, where it gives an incorrect energy spectrum.

The second unusual aspect of linear spectroscopy with the KMM eigenstates is the presence of finite oscillator strengths to manifolds of states with multiple excitations. As explained above and also noted in earlier work focused exclusively on the weak coupling regime [5, 6], such excitations are not allowed in the HL description and are a signature of the double excitation and de-excitation terms, $P_m^\dagger P_{m+1}^\dagger$ and $P_m P_{m+1}$, in Eq. (1). Our spectroscopic analysis allows one to extract the contribution of a manifold with any given number of excitations to the total oscillator strength. Specifically, oscillator strengths from the ground state $|\Phi_+\rangle$ to higher excitation number manifolds, i.e., χ_{2n+1} (weak coupling) and χ_{2n} (strong coupling) can be shown to possess the same linear M scaling and critical exponent $-3/4$ as χ_1. Since the number of states in these manifolds is large (e.g., 19900(1313400) two(three)-excitation states for $M = 200$), we sum over individual transitions in a given k and E interval to obtain a linear absorption density per unit momentum transfer and energy, $\rho_A(k,E)$, which displays the key features of the multi-excitation transitions. Figure 2 shows $\rho_A(k,E)$ from ground state to the three-excitation manifold ($B < 1$) and two-excitation manifold ($B > 1$) for

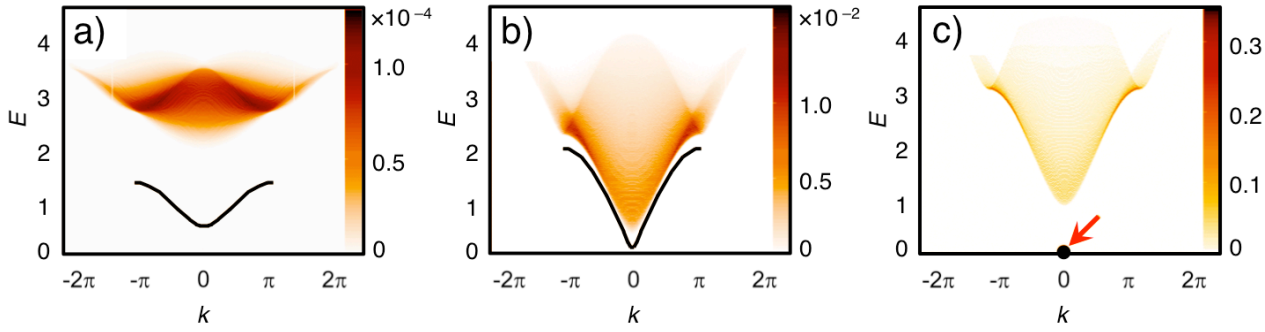

FIG. 2: Linear absorption density $\rho_A(k,E)$ from the ground state $|\Phi_+\rangle$ of an array with $M = 200$: to the three-excitation manifold, $G^\dagger(\alpha_1)G^\dagger(\alpha_2)G^\dagger(\alpha_3)|\Phi_-\rangle$, for $B = 0.40$ (a) and 0.90 (b); to the two-excitation manifold, $G^\dagger(\alpha_1)G^\dagger(\alpha_2)|\Phi_-\rangle$, for $B = 1.40$ (c). Black lines in panels (a) and (b) indicate the location of the one-excitation manifold, $G^\dagger(\alpha_1)|\Phi_-\rangle$. In the strong coupling regime the lowest excitation manifold collapses to a single transition $|\Phi_+\rangle \longrightarrow |\Phi_-\rangle$, indicated in panel (c) by the black dot and red arrow. Energy is in units of ε; wavenumber is in radians per lattice constant of the chromophore array.

an array of $M = 200$ chromophores. Additional results and the details of the (k,E) discretization can be found in [7].

Just as for absorption to the single-excitation manifold, the multi-excitation absorption is seen to be very different in the strong and weak coupling regimes. In the weak coupling regime (Figure 2a,b) the absorption density from the ground state, $|\Phi_+\rangle$, to three-excitation states, $G^\dagger(\alpha_3)G^\dagger(\alpha_2)G^\dagger(\alpha_1)|\Phi_-\rangle$, increases with B (note the different range of the color bar scale for panels (a) and (b)). While the transitions with maximum oscillator strength are always located at $k = 0$ for $b < 0$, the maximum value of $\rho_A(k,E)$ is nevertheless located close to $k = \pm\pi$ as a result of the higher density of states there. At the critical point $B = 1$, the parity of the eigenstates of H_- changes (see above) so that in the strong coupling regime transitions from $|\Phi_+\rangle$ to the two-excitation manifold, $G^\dagger(\alpha_1)G^\dagger(\alpha_2)|\Phi_-\rangle$ are now allowed (Figure 2c). In contrast to the weak coupling regime, as B now increases beyond unity, transitions to the higher-excitation manifolds are increasingly suppressed until $|\Phi_+\rangle \to |\Phi_-\rangle$ becomes the only allowed transition and saturates the oscillator strength. Because of the asymptotic degeneracy of $|\Phi_\pm\rangle$, the transition frequency further decreases to zero as M increases, implying again strong absorption and hyperradiance at arbitrarily low energies.

The exact treatment presented here shows that not only will significantly different linear spectra be found in weak and strong coupling regimes as a result of the different many-body nature of the corresponding energy eigenstates, but also that a unique linear spectral signature is associated with the quantum critical point at $B = 1$. Of particular note are the divergent oscillator strength at the critical point and superradiance exceeding the maximal one-photon rates, i.e., hyperradiance, found for $B > 1$. In this strong-coupling regime, the KMM model manifests long-range ordering of the transition dipole moments as $M \to \infty$. (It should be noted that in $d = 1$ quantum fluctuations do not necessarily destroy long range order, whereas $d \geq 2$ is needed to stabilize ordered states against thermal fluctuations.) Writing $|\Phi_\pm\rangle = (|+\rangle \pm |-\rangle)/\sqrt{2}$, where $P_M|+\rangle = |-\rangle$ and $\langle +|\sigma_1^x|+\rangle \to \left(1 - 1/B^2\right)^{1/8}$ as $M \to \infty$, we note that excitations are formed by introducing domains of reversed polarization which result from applying pairs of local "flip" operators. Excitations are thus generated in pairs in the strong coupling regime: the fact that only even numbers are allowed here is a topological constraint imposed by the cyclic boundary conditions.

While natural light harvesting systems, with electronic transition energies $> 10^4$ cm^{-1} and typical dipole-dipole interactions of order ~ 100 cm^{-1}, appear generally restricted to the weak coupling regime [5], we believe that the existence of a strong coupling region of parameter space with the spectral signatures we have described here may be a common feature of multi-chromophore systems. Both higher electronic states of neutral molecules [6] and polar molecules offer systematically larger effective interactions and consequently considerably larger values of B [18]. Further possibilities are suggested by quantum emulation of Eq. (1) using ultra cold dipolar molecules trapped in the sites of an optical lattice [19], capacitively coupled flux qubits [20] or trapped ions [21]. In particular, the strong pulse mediated alignment scheme of Ref. [19] enables controlled preparation of a chromophore array absorbing in the microwave regime with ε continuously tunable to zero, allowing emulation of the entire strong coupling regime and suggesting potential opportunities for high-efficiency detection of low energy photons.

More immediately, we note that the theoretical methods presented here provide a consistent, unifying treatment for all values of B that may be readily extended to analysis of non-linear spectroscopy for dipole-coupled chromophore arrays with arbitrary coupling strength [22].

A.A.K. acknowledges the financial support of The

Netherlands Organization for Scientific Research (NWO) Rubicon Grant 680-50-1022. K.B.W., J. D. and D.B.A. were supported by the DARPA QuBE program, B.A. and F. H. by NSF. We thank the Kavli Institute for Theoretical Physics for hospitality and for supporting this research in part by the National Science Foundation Grant No. PHY11-25915.

[1] F. C. Spano and S. Mukamel, J. Chem. Phys. **91**, 683 (1989).
[2] H. Fidder, J. Knoester, and D. A. Wiersma, J. Chem. Phys. **95**, 7880 (1991).
[3] J. I. Krugler, C. G. Montgomery, and H. M. McConnell, J. Chem. Phys. **41**, 2421 (1964).
[4] F. C. Spano, Phys. Rev. Lett. **67**, 3424 (1991).
[5] L. D. Bakalis and J. Knoester, J. Chem. Phys. **106**, 6964 (1997).
[6] V. Agranovich and D. Basko, J. Chem. Phys. **112**, 8156 (2000).
[7] See Supplemental Material at http://link.aps.org/supplemental/ xx.xxxx/PhysRevZ.xx.xxxxxx.
[8] B. McCoy, Phys. Rev. **173**, 531 (1968).
[9] For M even, all results for $b > 0$ may be obtained by applying a rotation about the z axis through π on either of the two sublattices. The case of M odd is complicated by the periodic boundary conditions and will be considered elsewhere.
[10] D. B. Abraham, J. Math. Phys. **53**, 095224 (2012).
[11] E. R. Caianiello, *Combinatorics and Renormalization in Quantum Field Theory* (W. A. Benjamin, 2003).
[12] W. H. Press, S. A. Teukolsky, W. T. Vetterling, and B. P. Flannery, *Numerical Recipies in C: The Art of Scientific Computing* (Cambridge University Press, 1992), 2nd ed.
[13] The computational complexity of solving Eqs. (4) and (5) is $\propto M^3$, significantly better than for directly diagonalizing the complete KMM Hamiltonian, Eq. (1) ($\propto 2^{3M}$ [12]). It is the same as for diagonalization of the one-excitation subspace in the HL approximation.
[14] M. O. Scully and A. A. Svidzinsky, Science **325**, 1510 (2009).
[15] In the HL approximation the total oscillator strength scales with M: with periodic boundary conditions the $\alpha = 0$ state saturates this while with fixed boundary conditions the corresponding lowest (for $b < 0$) energy state contains $\sim 81\%$ of the total oscillator strength [2].
[16] R. Dicke, Phys. Rev. **93**, 99 (1954).
[17] N. Grønbech-Jensen and J. A. Blackburn, Phys. Rev. Lett. **70**, 1251 (1993).
[18] F. Terenziani and A. Painelli, Phys. Rev. B **68**, 165405 (2003).
[19] F. Herrera, S. Kais, and K. B. Whaley, arXiv preprint arXiv:1302.6444 (2013).
[20] S. Mostame, P. Rebentrost, A. Eisfeld, A. J. Kerman, D. I. Tsomokos, and A. Aspuru-Guzik, New J. Phys. **14**, 105013 (2012).
[21] R. Islam, E. Edwards, K. Kim, S. Korenblit, C. Noh, H. Carmichael, G.-D. Lin, L.-M. Duan, C.-C. J. Wang, J. Freericks, et al., Nature Comm. **2**, 377 (2011).
[22] A.A. Kocherzhenko, J. Dawlaty, D.B. Abraham, K.B. Whaley. To be published.